A two-dimensional numerical procedure for a three dimensional internal flow through a complex passage with a small depth (its application to numerical analysis of fluidic oscillators)

A. Nakayama, F. Kuwahara and Y. Kamiya
Department of Mechanical Engineering, Shizuoka University, Hamamatsu, Japan

Received April 2004
Revised September 2004
Accepted October 2004

Abstract

Purpose – To introduce an efficient two-dimensional numerical procedure for a three-dimensional internal flow through a complex passage with a small depth, in which the viscous effects from upper and lower walls are significant.

Design/methodology/approach – A set of two-dimensional governing equations has been derived by integrating the full three-dimensional Navier-Stokes equations over the depth. Then, this set of the governing equations has been discretized using a finite volume method. *Simple* algorithm and *quick* scheme are used to solve the resulting discretized equations.

Findings – A numerical experiment conducted to investigate the oscillation mechanism of a feedback fluidic oscillator reveals that the feedback passage plays an important role of transmitting the pressure rise to the control port, which triggers the jet stream to deflect towards the opposite side wall in the reaction region. Comparison of the prediction and experiment substantiates the validity of the present numerical procedure.

Originality/value – The two-dimensional numerical procedure, proposed in this study, will be used by researchers and practitioners to investigate various kinds of complex passages with a small depth. Especially, those who are interested in fluidic devices may find it extremely convenient to conduct numerical experiments.

Keywords Flow, Numerical analysis, Oscillations

Paper type Research paper

Nomenclature

f	= velocity profile function	$\bar{u}, \bar{v}$	= average velocity components
$h(x, y)$	= half depth of the passage, function for the wall geometry	u_{in}	= bulk mean velocity at the nozzle inlet
u, v, w	= velocity components in the x, y and z directions	p	= pressure
		$Re_{L_{in}} = (u_{in}L_{in})/\nu$	= Reynolds number based on L_{in} and u_{in}

The authors would like to express their sincere thanks to President Morikawa, Technical Division Head Kageyama and Senior Researcher Tsukamoto of Nihon Biniron Co., Hamamatsu, Japan, for their support.

International Journal of Numerical Methods for Heat & Fluid Flow
Vol. 15 No. 8, 2005
pp. 863-871

0961-5539
DOI 10.1108/09615530510625129

$St = (fL_{in})/u_{in}$	= Strouhal number	$\zeta = z/(h(x,y))$	= dimensionless coordinate
t	= time		
x, y, z	= Cartesian coordinates		
ν	= kinematic viscosity	*Subscript*	
ρ	= density	in	= nozzle inlet

Introduction

Recent advances in microfabrication technologies have been so promising that some micro-fluidics may compete with conventional mechanical and electrical systems. Fluidic devices such as feedback fluidic oscillators (Zemel and Furlan, 1996; Parry *et al.*, 1991; Trippetts *et al.*, 1973) and fluidic flowmeters (Lua and Zheng, 2003; Mansy and Williams, 1989; Boucher and Mazharoglu, 1988) consist of complex three-dimensional passages. Numerical studies on such fluidic devices are essential to reveal flow characteristics and to find their optimal geometrical parameters for designing.

Figure 1 shows a typical feedback fluidic oscillator used for spraying water to the automobile windshield. This type of devise in general has four functional elements, namely, supply port, control ports, output port and interacting region, as indicated in the figure. The depth of flow passages is comparatively small as compared with the device width and its loop length. Because of geometrical complexities, we usually have to be content with undertaking only two-dimensional numerical analyses for flows through such fluidic devices (Uzol and Camci, 2001; Lua and Zheng, 2003). However, the validity of such two-dimensional computational results becomes questionable when the depth of flow passages is so small that the viscous forces resulting from both upper and lower walls are not negligible.

In this paper, we shall propose a novel two-dimensional numerical procedure for analyzing a three-dimensional internal flow through a complex passage with a small

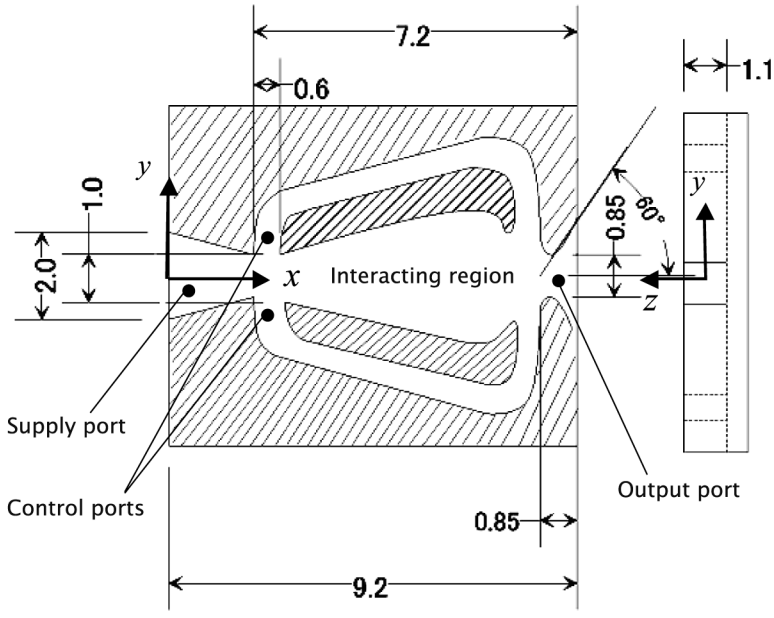

Figure 1.
Fluidic oscillator

depth. Unlike conventional two-dimensional schemes, the viscous effects of upper and lower walls on the oscillating flow are fully taken into consideration. We derive the two-dimensional governing equations by integrating full Navier-Stokes equations in a three-dimensional form, over the channel depth, and then retaining the wall shear terms associated with the upper and lower walls. The resulting two-dimensional governing equations are discretized and numerically solved using *simple* algorithm coupled with *quick* scheme. The fluidic oscillator as shown in Figure 1 is studied numerically under possible operating conditions for spraying water to the automobile windshield. The results of oscillating frequency are compared with the experimental data, which substantiates the validity of this economical numerical procedure and its acquired accuracy.

Two-dimensional Navier-Stokes equation integrated over the depth

Usually, the flow within the passage stays laminar since the depth is so small. The continuity and Navier-Stokes equations for incompressible flows are given by:

$$\frac{\partial u}{\partial x}+\frac{\partial v}{\partial y}+\frac{\partial w}{\partial z}=0 \tag{1}$$

$$\frac{\partial u}{\partial t}+\frac{\partial}{\partial x}\left(u^2-\nu\frac{\partial u}{\partial x}\right)+\frac{\partial}{\partial y}\left(vu-\nu\frac{\partial u}{\partial y}\right)+\frac{\partial}{\partial z}\left(wu-\nu\frac{\partial u}{\partial z}\right)=-\frac{1}{\rho}\frac{\partial p}{\partial x} \tag{2}$$

$$\frac{\partial v}{\partial t}+\frac{\partial}{\partial x}\left(uv-\nu\frac{\partial v}{\partial x}\right)+\frac{\partial}{\partial y}\left(v^2-\nu\frac{\partial v}{\partial y}\right)+\frac{\partial}{\partial z}\left(wv-\nu\frac{\partial v}{\partial z}\right)=-\frac{1}{\rho}\frac{\partial p}{\partial y} \tag{3}$$

$$\frac{\partial w}{\partial t}+\frac{\partial}{\partial x}\left(uw-\nu\frac{\partial w}{\partial x}\right)+\frac{\partial}{\partial y}\left(vw-\nu\frac{\partial w}{\partial y}\right)+\frac{\partial}{\partial z}\left(w^2-\nu\frac{\partial w}{\partial z}\right)=-\frac{1}{\rho}\frac{\partial p}{\partial z} \tag{4}$$

The passage in consideration is symmetric with respect to the x-y plane such that the upper and lower wall geometries are given by $z=\pm h(x,y)$, respectively. The following procedure appears to be similar to that of Hele-Shaw flow. However, it is noted that $h(x, y)$ can vary spatially, and that both inertial and viscous terms are retained. Integrating the continuity equation from 0 to $h(x, y)$ with respect to z as:

$$\frac{\partial}{\partial x}\int_0^h u\,\mathrm{d}z+\frac{\partial}{\partial y}\int_0^h v\,\mathrm{d}z=0 \tag{5}$$

Assuming the velocity profiles as:

$$u(t,x,y,z)=\bar{u}(t,x,y)f(\zeta)\ \text{ and }\ v(t,x,y,z)=\bar{v}(t,x,y)f(\zeta) \tag{6}$$

where

$$\zeta=\frac{z}{h(x,y)} \tag{7}$$

and $\bar{u}(x,y)$ and $\bar{v}(x,y)$ are the velocity components averaged over the depth, such that the symmetric function $f(\zeta)$ should satisfy:

$$f(\pm1)=0,\quad f'(0)=0\ \text{ and }\ \int_0^1 f\,\mathrm{d}\zeta=1 \tag{8}$$

The foregoing integral form of the continuity equation (5) may be rewritten as:

$$\frac{\partial \bar{u}h}{\partial x} + \frac{\partial \bar{v}h}{\partial y} = 0 \tag{9}$$

Furthermore, substituting the foregoing velocity profiles into the original form of the continuity equation (1) as:

$$\begin{aligned} \frac{\partial w}{\partial z} &= -f\left(\frac{\partial \bar{u}}{\partial x} + \frac{\partial \bar{v}}{\partial y}\right) + \frac{\zeta f'}{h}\left(\bar{u}\frac{\partial h}{\partial x} + \bar{v}\frac{\partial h}{\partial y}\right) = \frac{(\zeta f)'}{h}\left(\bar{u}\frac{\partial h}{\partial x} + \bar{v}\frac{\partial h}{\partial y}\right) \\ &\leq (\zeta f)'\frac{\sqrt{\bar{u}^2 + \bar{v}^2}}{h}\sqrt{\left(\frac{\partial h}{\partial x}\right)^2 + \left(\frac{\partial h}{\partial y}\right)^2} \end{aligned} \tag{10}$$

We suppose that the function $h(x,y)$ varies gradually such that:

$$\left|\frac{\partial h}{\partial x}\right| \ll 1 \text{ and } \left|\frac{\partial h}{\partial y}\right| \ll 1 \tag{11}$$

Since $(\zeta f)'$ is of the order of unity, the foregoing equation (10) leads to:

$$\left|\frac{\partial w}{\partial z}\right| \ll \frac{\sqrt{\bar{u}^2 + \bar{v}^2}}{h} \tag{12}$$

and hence, we have:

$$w(x, y, z) \simeq 0 \tag{13}$$

Then, the z-momentum equation (4) immediately gives:

$$p = p(t, x, y) \tag{14}$$

We substitute the velocity profiles and pressure given by equations (6) and (14) into the x- and y-momentum equations (2) and (3), and then integrate them over the depth to find:

$$\begin{aligned} &h\frac{\partial \bar{u}}{\partial t} + \frac{\partial}{\partial x}\left(h\left(\bar{u}^2 - \nu\frac{\partial \bar{u}}{\partial x}\right)\right) + \frac{\partial}{\partial y}\left(h\left(\bar{v}\bar{u} - \nu\frac{\partial \bar{u}}{\partial y}\right)\right) \\ &\quad = -\frac{h}{\rho}\frac{\partial p}{\partial x} + \nu f'(1)\frac{\bar{u}}{h}\left(1 + \frac{\partial h}{\partial x} + \frac{\partial h}{\partial y}\right) \end{aligned} \tag{15}$$

$$\begin{aligned} &h\frac{\partial \bar{v}}{\partial t} + \frac{\partial}{\partial x}\left(h\left(\bar{u}\bar{v} - \nu\frac{\partial \bar{v}}{\partial x}\right)\right) + \frac{\partial}{\partial y}\left(h\left(\bar{v}^2 - \nu\frac{\partial \bar{v}}{\partial y}\right)\right) \\ &\quad = -\frac{h}{\rho}\frac{\partial p}{\partial y} + \nu f'(1)\frac{\bar{v}}{h}\left(1 + \frac{\partial h}{\partial x} + \frac{\partial h}{\partial y}\right) \end{aligned} \tag{16}$$

where the Leibnitz rule and no-slip conditions are exploited as:

$$\int_0^{h(x,y)} \frac{\partial}{\partial x}\left(u\phi - \nu\frac{\partial\phi}{\partial x}\right) \mathrm{d}z = \frac{\partial}{\partial x}\int_0^{h(x,y)} \left(u\phi - \nu\frac{\partial\phi}{\partial x}\right) \mathrm{d}z - \left(u\phi - \nu\frac{\partial\phi}{\partial x}\right)_{z=h}\frac{\partial h}{\partial x}$$
$$\simeq \frac{\partial}{\partial x}\left(h\left(\bar{u}\bar{\phi} - \nu\frac{\partial\bar{\phi}}{\partial x}\right)\right) + \nu\frac{\partial\bar{\phi}}{\partial x}\bigg|_{z=h}\frac{\partial h}{\partial x}$$
$$= \frac{\partial}{\partial x}\left(h\left(\bar{u}\bar{\phi} - \nu\frac{\partial\bar{\phi}}{\partial x}\right)\right) - \nu f'(1)\frac{\bar{\phi}}{h}\frac{\partial h}{\partial x}$$

Likewise

$$\int_0^{h(x,y)} \frac{\partial}{\partial y}\left(v\phi - \nu\frac{\partial\phi}{\partial y}\right) \mathrm{d}z = \frac{\partial}{\partial y}\left(h\left(\bar{v}\bar{\phi} - \nu\frac{\partial\bar{\phi}}{\partial y}\right)\right) - \nu f'(1)\frac{\bar{\phi}}{h}\frac{\partial h}{\partial y}$$

and

$$\int_0^{h(x,y)} \frac{\partial}{\partial z}\left(w\phi - \nu\frac{\partial\phi}{\partial z}\right) \mathrm{d}z = -\nu f'(1)\frac{\bar{\phi}}{h}$$

The foregoing function ϕ may be either u or v. When the function $h(x, y)$ is moderate enough to satisfy the condition given by equation (11), the integrated momentum equations (15) and (16) reduce to:

$$h\frac{\partial\bar{u}}{\partial t} + \frac{\partial}{\partial x}\left(h\left(\bar{u}^2 - \nu\frac{\partial\bar{u}}{\partial x}\right)\right) + \frac{\partial}{\partial y}\left(h\left(\bar{v}\bar{u} - \nu\frac{\partial\bar{u}}{\partial y}\right)\right) = -\frac{h}{\rho}\frac{\partial p}{\partial x} - 3\nu\frac{\bar{u}}{h} \qquad (17)$$

$$h\frac{\partial\bar{v}}{\partial t} + \frac{\partial}{\partial x}\left(h\left(\bar{u}\bar{v} - \nu\frac{\partial\bar{v}}{\partial x}\right)\right) + \frac{\partial}{\partial y}\left(h\left(\bar{v}^2 - \nu\frac{\partial\bar{v}}{\partial y}\right)\right) = -\frac{h}{\rho}\frac{\partial p}{\partial y} - 3\nu\frac{\bar{v}}{h} \qquad (18)$$

where one of the simplest candidates for the symmetric function $f(\zeta)$ is assumed as:

$$f(\zeta) = \frac{3}{2}(1 - \zeta^2) \qquad (19)$$

to conform with the no-slip and symmetry conditions given by equation (8). The integrated momentum equations (17) and (18) along with the integrated continuity equation (9) form a complete set of the governing equations for a three-dimensional internal flow through a complex passage with a small depth. These governing equations subject to no-slip conditions are believed to be valid for all passages described by a moderately varying arbitrary function $h(x, y)$. In this study, however, only the fluidic oscillator with constant h, as shown in Figure 1, will be examined numerically.

Numerical calculation procedure

The governing equations (17), (18) and (9) were integrated over a small element and time interval, so as to establish a set of the discretized equations. The well-known quick scheme has been adopted for differencing the advection terms. Then, they were numerically solved using simple algorithm proposed by Patankar and Spalding (1972). Convergence was measured in terms of the maximum change in each variable during an iteration. The maximum change allowed for the convergence check was set to 10^{-5}, as the variables are normalized by appropriate references. Further details on this numerical procedure can be found in Patankar (1980) and Nakayama (1995).

A typical grid system consists of 201 × 201 nodes with dense and coarse meshes for the regions inside and outside of the passages, respectively, to cover a large domain of integration, including both the fluidic devise and its surroundings, namely, 100 × 25 mm. Figure 2 shows a part of dense mesh distributed around the fluidic oscillator for the present non-uniform grid system. Preliminary calculations were made to compare the results against those obtained with 301 × 301 nodes for some selected cases. In this way, the originally used grid resolution was found sufficient. Moreover, the time step was set small enough to satisfy Courant condition, after confirming that any further decrease in the time step does not alter the results significantly.

In this study, the Cartesian grid system is used instead of the body fitted system. The latter is recommended if the detailed flow field within the passage needs to be explored. However, when only macroscopic characteristics such as oscillation frequency are needed, the former would suffice for the purpose. All computations were performed using the computer system at Shizuoka University Computer Center.

Results and discussion

The fluidic oscillator under investigation, as shown in Figure 1, is one of typical fluidic devices installed in Japanese automobiles for spraying water to the windshield. Experimental investigation has been also conducted to measure the frequency of oscillating flow by a stroboscope. The bulk mean velocity u at the nozzle inlet was varied from 2.2 to 6.0 m/s, by controlling the voltage of the battery from 5 to 10 V. For this operation range, the Reynolds number $Re_{L_{\text{in}}}$ based on the inlet width L_{in} and velocity u varies from 4,400 to 12,000.

Numerical computations were carried out for the same operation range by feeding the uniform velocity at the inlet. It takes about ten cycles of oscillations for the velocity to attain its periodically, fully-developed stage. Figure 3 (a)-(f) depict a complete cycle of the periodically fully-developed velocity field for the case of $Re_{L_{\text{in}}} = 4,400$, while Figure 4 shows the corresponding signals of the oscillating velocity components, obtained at the selected point P indicated in Figure 2. These figures clearly show that the oscillation frequency for this case is about $f = 1/25\,\text{ms} = 40\,\text{Hz}$.

As shown in Figure 3(a), the Coanda effect tends to deflect the jet stream towards the upper wall in the reacting region. The lower pressure region formed between this deflected stream and the upper wall keeps the jet stream deflected. Because of this

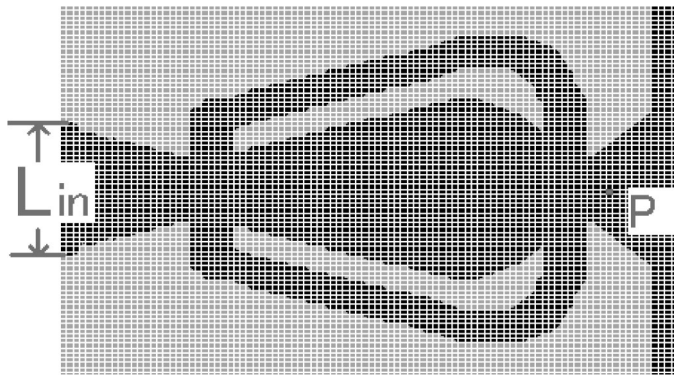

Figure 2.
Mesh around a fluidic oscillator

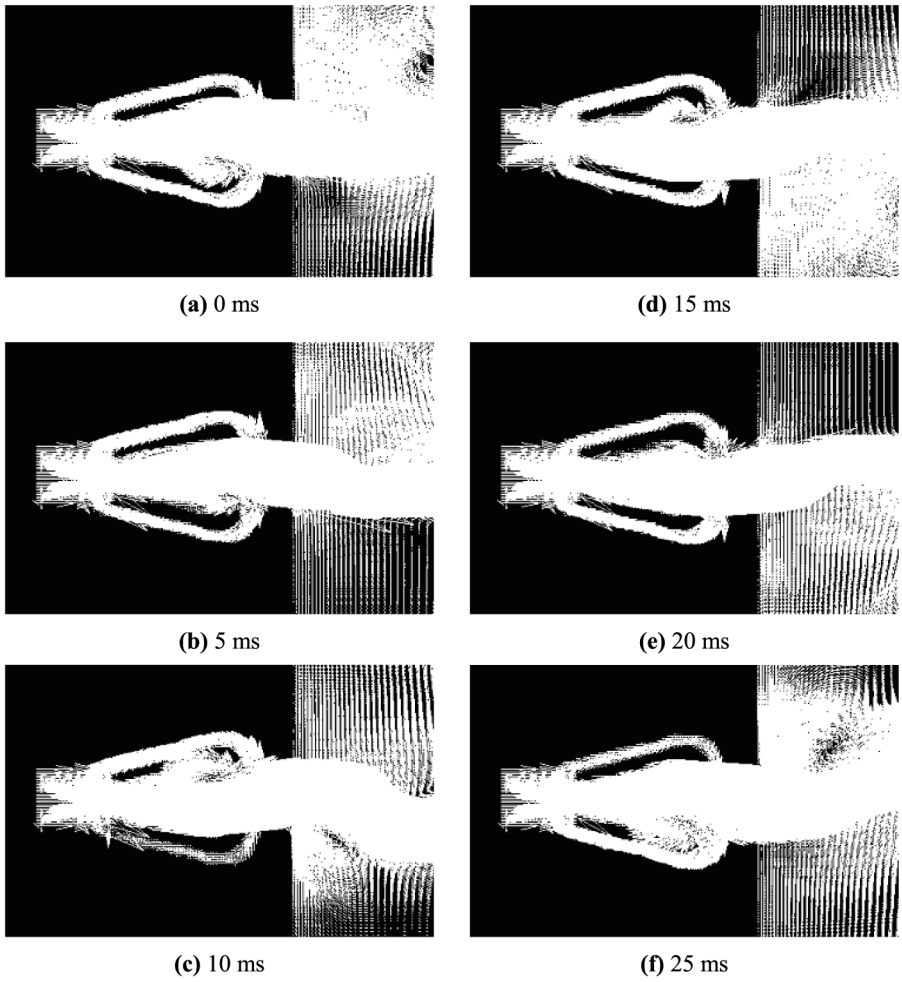

Figure 3.
Predicted oscillating velocity field

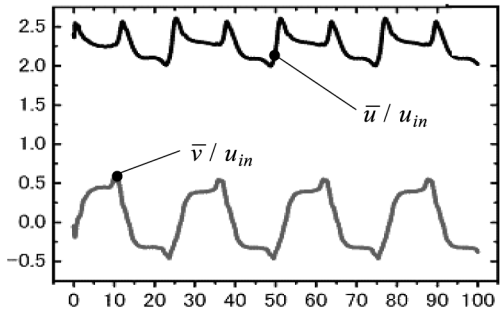

Figure 4.
Predicted temporal variation of velocity components

deflection, the fluid tends to impinge onto the upper feedback port, upstream of the output port, transmitting the pressure rise back to the control port by the speed of sound through the outer feedback passage (Figure 3(b)). Then, the transmitted pressure rise triggers the jet stream to bend towards the opposite (lower) wall (Figure 3(c)). This sequence is repeated with the stream deflected towards the lower wall so as to form a complete cycle of oscillation (Figure 3(d)-(f)). It is interesting to see from Figure 4 that the jet stream changes its direction so quickly as the velocity either decreases or increases within 5 ms. The swift change in the jet direction may also be appreciated from Figure 3(b) and (c), and also from Figure 3(e) and (f). This trend of swift switching has been confirmed visually from the experiment.

The foregoing observation prompts us to wonder if the jet would still oscillate when the outer feedback passages are taken off. Thus, another series of computations were conducted for such cases, as shown in Figure 5 for a typical case of $Re_{L_{\text{in}}} = 4,400$. The figure shows that the jet is under the influence of the Coanda effect, yet, no oscillations were observed for the range of Reynolds number studied here.

The results of computations carried out for the fluidic oscillator are assembled in terms of Strouhal number $St \equiv fL_{\text{in}}/u_{\text{in}}$, and are plotted in Figure 6, along with the experimental data. The predicted Strouhal number St stays almost constant, namely,

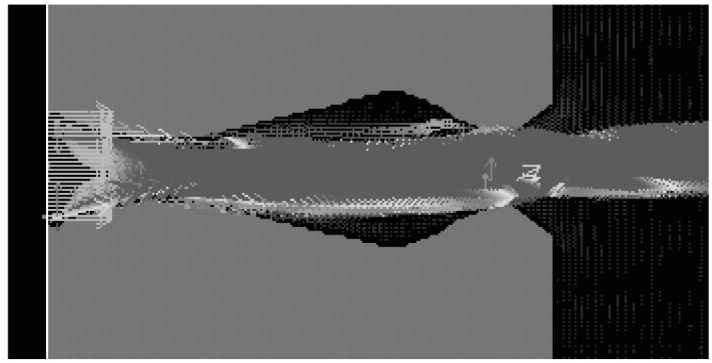

Figure 5.
Predicted velocity field for the case without feedback passages

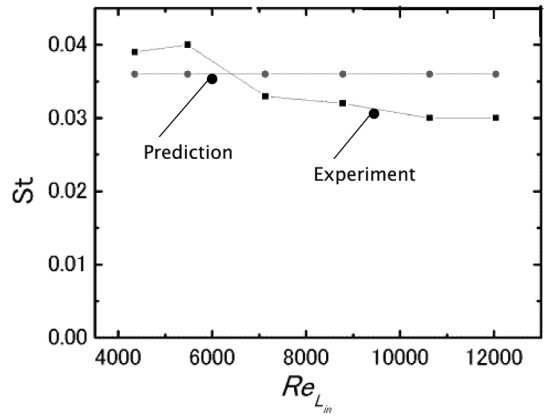

Figure 6.
Effect of Reynolds number on Strouhal number

$St \equiv fL_{in}/u_{in} = 0.36$, over this range of Reynolds number, while that of the experiment decreases around $Re_{L_{in}} = 6,000$. However, both levels of St are quite close, which substantiates the validity of the present two-dimensional numerical procedure. As increasing the Reynolds number, the flow may have become turbulent. However, the mechanism of the fluidic oscillation explained above holds even for the case of turbulent jets.

Concluding remarks

An efficient two-dimensional numerical calculation procedure has been proposed for a three dimensional internal flow through a complex passage with a small depth, in which the viscous forces acting on both upper and lower walls are so significant that they cannot be neglected. A set of two-dimensional governing equations has been derived by integrating the full three-dimensional Navier-Stokes equation over the depth. Then, this set of the governing equations was discretized using a finite volume method, so as to confirm with simple algorithm. A numerical experiment has been conducted to investigate the oscillation mechanism of a feedback fluidic oscillator, which is designed to spray water to an automobile windshield. It has been found that the feedback passage plays an important role of transmitting the pressure rise to the control port, which triggers the jet to deflect towards the opposite side wall in the reaction region. The Strouhal number predicted by the present numerical procedure is in good accord with that of the experiment, which proves the validity of the present economical numerical procedure.

References

Boucher, R.F. and Mazharoglu, C. (1988), "Low Reynolds number fluidic flowmetering", *Journal of Physics, E: Scientific Instruments*, Vol. 21, pp. 977-89.

Lua, A.C. and Zheng, Z. (2003), "Numerical simulations and experimental studies on a target fluidic flow meter", *Flow Measurement and Instrumentation*, Vol. 14, pp. 43-9.

Mansy, H. and Williams, D.R. (1989), "An experimental and numerical study of trapped vortex pair fluidic flowmeter", *ASME FED Forum on Turbulent Flows*, Vol. 76, pp. 35-9.

Nakayama, A. (1995), *PC-Aided Numerical Heat Transfer and Convective Flow*, CRC Press, Boca Raton, FL.

Parry, A.J., Chiwanga, S.G., Kalsi, H.S. and Jepson, P. (1991), "Numerical and experimental visualization of flow through a target fluidic oscillator", *ASME FED Experimental and Numerical Flow Visualization*, Vol. 128, pp. 327-34.

Patankar, S.V. (1980), *Numerical Heat Transfer and Fluid Flow*, Hemisphere, Washington, DC.

Patankar, S.V. and Spalding, D.B. (1972), "A calculation procedure for heat, mass and momentum transfer in three-dimensional parabolic flows", *International Journal of Heat Mass Transfer*, Vol. 15, pp. 1787-806.

Trippetts, J.R., Ng, H.K. and Royle, J.K. (1973), "An oscillating bistable fluid amplifier for use as a flowmeter", *Fluidics Quarterly*, Vol. 5 No. 1.

Uzol, O. and Camci, C. (2001), "Experimental and computational visualization and frequency measurements of the jet oscillation inside a fluidic oscillator", paper presented at Fourth International Symposium on Particle Image Velocimetry, Gottingen, PIV'01 Paper 1029, September 17-19, pp. 1-9.

Zemel, J.N. and Furlan, R. (1996), "Microfluidics", in Taylor, R.F. and Schultz, J.S. (Eds), *Handbook of Chemical and Biological Sensors*, Institute of Physics Publishing, Bristol and Philadelphia, pp. 317-47.